

ELECTRIC QUADRUPOLE AND HEXADECAPOLE MOMENTS IN THE TRANSITIONAL NUCLEI ^{150}Nd , ^{152}Sm , ^{154}Sm , ^{154}Gd AND ^{156}Gd †

H. J. WOLLERSHEIM and Th. W. ELZE

Institut für Kernphysik der Universität Frankfurt, Frankfurt/Main, Germany

Received 3 September 1976

(Revised 10 November 1976)

Abstract: Electric quadrupole and hexadecapole transition matrix elements were measured for ^{150}Nd , ^{154}Gd and ^{156}Gd in Coulomb excitation experiments with ^4He projectiles. The measured excitation probabilities are analyzed in the framework of the rotation-vibration coupling model. The following reduced E2 and E4 transition matrix elements are obtained for ^{150}Nd , ^{154}Gd and ^{156}Gd , respectively: $\langle 2^+ || M(E2) || 0^+ \rangle = 1.650 \pm 0.012 e \cdot b$, $1.958 \pm 0.011 e \cdot b$, $2.142 \pm 0.020 e \cdot b$; and $\langle 4^+ || M(E4) || 0^+ \rangle = 0.30^{+0.06}_{-0.07} e \cdot b^2$, $0.64^{+0.06}_{-0.07} e \cdot b^2$, $0.41^{+0.12}_{-0.18} e \cdot b^2$. Previous Coulomb excitation experiments performed in this laboratory are also analyzed using this model and yield the following results for ^{152}Sm and ^{154}Sm , respectively: $\langle 2^+ || M(E2) || 0^+ \rangle = 1.864 \pm 0.017 e \cdot b$, $2.072 \pm 0.010 e \cdot b$; and $\langle 4^+ || M(E4) || 0^+ \rangle = 0.46 \pm 0.08 e \cdot b^2$, $0.57 \pm 0.09 e \cdot b^2$. Charge deformation parameters, β_2 and β_4 , are deduced from the measured transition moments.

E

NUCLEAR REACTIONS $^{150}\text{Nd}(\alpha, \alpha')$, $E = 11.5$ MeV, $^{154,156}\text{Gd}(\alpha, \alpha')$, $E = 11.8$ MeV; measured (E_α , 160°); deduced reduced matrix elements $\langle 2^+ || M(E2) || 0^+ \rangle$, $\langle 4^+ || M(E4) || 0^+ \rangle$ and charge deformation parameters β_2 , β_4 .

1. Introduction

The Coulomb excitation process has been frequently used to measure precisely quadrupole and hexadecapole moments of even deformed nuclei in both the rare earth and actinide regions of the periodic table¹⁻¹¹). In such experiments the excitation probabilities of the 2^+ and 4^+ ground-band rotational levels are usually determined by either detecting the elastically and inelastically scattered projectiles or by measuring the decay γ -rays. The data analysis is performed by calculating the 2^+ and 4^+ excitation probabilities by means of a suitable theory of Coulomb excitation as a function of all E2 and E4 matrix elements which connect the various levels. By comparison of the calculated excitation probabilities with experiment the reduced transition matrix elements $M_{02} = \langle 2^+ || M(E2) || 0^+ \rangle$ and $M_{04} = \langle 4^+ || M(E4) || 0^+ \rangle$ are determined. These matrix elements may then be used to deduce quadrupole (β_2) and hexadecapole (β_4) deformation parameters.

† Supported by the Bundesministerium für Forschung und Technologie.

Over a range of nuclei in both the rare earth and actinide region the rigid-rotor model has been successfully used to relate the $E\lambda$ matrix elements $M_{if} = \langle I_f || M(E\lambda) || I_i \rangle$ ($\lambda = 2, 4$) to $M_{0\lambda}$, thus leaving the two quantities M_{02} and M_{04} to be determined from experiment. In the transition region ($N \approx 90$), however, where the rotation-vibration coupling is strong and the nuclei behave like "soft" rotors, the rigid-rotor description is not applicable and a model should be employed which takes the rotation-vibration mixing into account.

In this paper we report the results of Coulomb excitation measurements of E2 and E4 transition matrix elements in the transitional nuclei ^{150}Nd , ^{152}Sm , ^{154}Sm , ^{154}Gd and ^{156}Gd . It will also be shown that relative ground-band E2 matrix elements in these nuclei as calculated within the framework of the rotation-vibration coupling model are in excellent agreement with results from recent experiments. Preliminary results were reported earlier¹²).

2. Experimental procedure

The experiments were performed by bombarding thin ($10\text{--}20 \mu\text{g}/\text{cm}^2$) targets of ^{150}Nd , ^{154}Gd , and ^{156}Gd with α -particles from the University of Frankfurt Van de Graaff accelerator. The beam energy was chosen to be 11.5 and 11.8 MeV for the ^{150}Nd and $^{154}, ^{156}\text{Gd}$ targets, respectively. The isotopic abundance of the target material used was $> 96\%$ for ^{150}Nd and ^{154}Gd , while the enrichment of the ^{156}Gd target was 93.6%. Elastically and inelastically scattered α -particles were detected $\theta_{\text{lab}} = 160^\circ$ with a cooled Si surface-barrier detector. The energy resolution was typically 19 keV, FWHM. A spectrum resulting from the $^{154}\text{Gd}(\alpha, \alpha')$ reaction is shown in fig. 1.

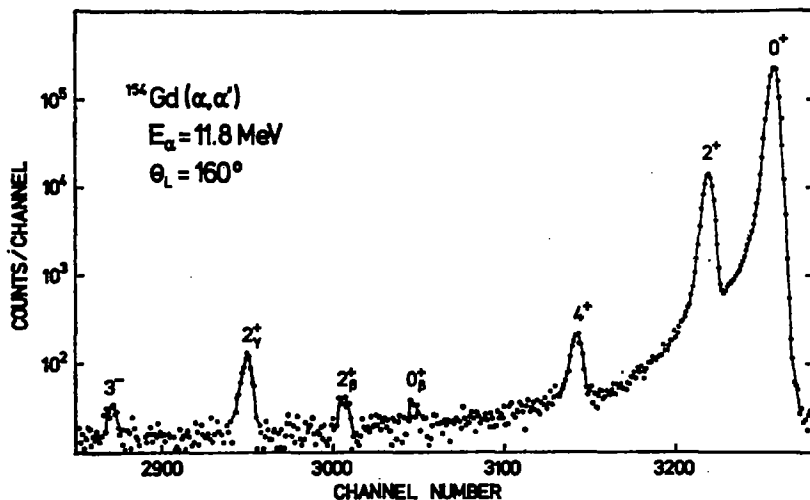


Fig. 1. Energy spectrum of 11.8 MeV α -particles scattered from ^{154}Gd .

The excitation cross section for the 2^+ state was determined by means of a computer code which separated the 2^+ and 0^+ peaks in a self-consistent iterative procedure assuming identical peak shapes. Simultaneously the intensities were corrected for the known impurities in the target material. The cross section of the 4^+ state was subsequently obtained by fitting a fourth-order polynomial to the background above and below the 4^+ peak. The statistical uncertainty associated with the 2^+ intensity is approximately 1.5 %, while the 4^+ cross section is believed to be accurate to within 3-4 %.

Other states at higher excitation energies than the 2^+ and 4^+ ground-band levels were also measured in our experiments, as can be seen in fig. 1. Among the higher states are the 2^+ γ -vibrational, 0^+ and 2^+ β -vibrational, and the 3^- octupole vibrational levels. Spectroscopic information on the vibrational states seen in the present experiment, together with results from previous work performed in this laboratory ^{7, 8}) will be given in a future publication ¹³).

3. Analysis and discussion

To obtain the reduced matrix elements $M_{02} = \langle 2^+ || M(E2) || 0^+ \rangle$ and $M_{04} = \langle 4^+ || M(E4) || 0^+ \rangle$ from the experimental data the Coulomb excitation cross sections of the 2^+ and 4^+ ground-band rotational states were calculated by means of a quantum mechanical coupled channel code ¹⁴). Included in these calculations were all E2 and E4 matrix elements which connect the 0^+ , 2^+ and 4^+ levels of the ground band. Higher states, i.e the 6^+ ground-band level, the β - and γ - vibrational states, as well as the 3^- octupole level are found to have very little influence on the excitation probabilities of the 2^+ and 4^+ ground-band rotational states and are neglected in the calculations.

To compute the reduced E2 and E4 matrix elements for the transitional nuclei studied here and relate them to M_{02} and M_{04} , respectively, a nuclear model must be used which takes account of the rotation-vibration interaction found in these nuclei. The E2 matrix elements were calculated employing both the rotation-vibration model (RVM) of Faessler and Greiner ¹⁵) and the Davydov-Ovcharenko model ¹⁶). For ¹⁵²Sm, the RVM calculations were performed by using the parameters $\epsilon = 32.2$ keV, $E_\gamma = 1039.4$ keV, $E_\beta = 684.6$ keV, while in the Davydov model parameters $\mu = 0.37$ and $\gamma = 11.5^\circ$ were used ¹⁷).

Appropriate parameters were used for the other nuclei studied. In fig. 2 (upper left display), the calculated ground-band $B(E2)$ values in ¹⁵²Sm, normalized to the $B(E2; 2^+ \rightarrow 0^+)$ value, are compared with experimental data ¹⁸). The $B(E2)$ values calculated from the rotation-vibration model are labeled RVM-1. Both the RVM-1 and the Davydov model yield $B(E2)$ values that agree better with experiment than do the corresponding rigid-rotor values. It is seen, however, that the theoretical $B(E2)$ values tend to be systematically larger than the experimental values. Similar results are obtained for ¹⁵⁴Sm, ¹⁵⁴Gd and ¹⁵⁶Gd, but are omitted from fig. 2 for

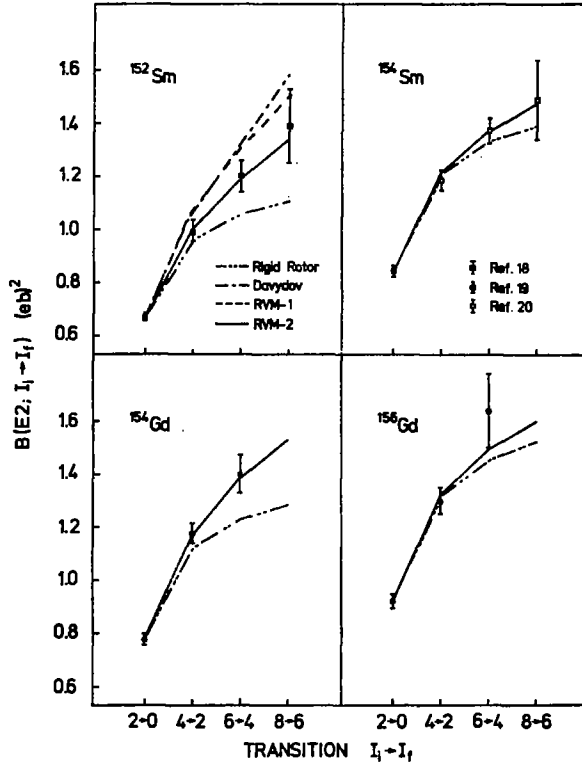


Fig. 2. The $B(E2)$ values between ground-band rotational states in rare earth nuclei.

clarity. For ^{150}Nd no ground-band $B(E2)$ values other than $B(E2; 2^+ \rightarrow 0^+)$ have been available to us.

In the case of the RVM-1 the observed deviations between theory and experiment may be due to two approximations made: (i) the charge distribution of the nucleus has been assumed to be homogeneous, and (ii) terms higher than quadratic have been neglected in the expansion of the nuclear surface in terms of the quadrupole deformation parameter β_2 . These higher-order terms contribute about 2% to the reduced E2 matrix element, while particularly the $\langle 4^+ || M(E2) || 2^+ \rangle$ element is often determined experimentally to within $\approx 1\%$. Since the hexadecapole matrix element $\langle 4^+ || M(E4) || 0^+ \rangle$ to be deduced from the present Coulomb excitation study is very sensitive to small changes in the two-step E2 strength, it appears to be desirable to improve the model calculations. Therefore, we have recalculated the E2 matrix elements within the framework of the rotation-vibration model. By expressing the transition matrix elements in terms of three "intrinsic" matrix elements, which may be obtained from experiment, the above-mentioned approximations in the RVM are avoided. Details of our calculations are given in the appendix. The $B(E2)$ values calculated in this way for ^{152}Sm , ^{154}Sm , ^{154}Gd and ^{156}Gd are compared with experi-

mental data ¹⁸⁻²⁰) in fig. 2. As can be seen, these calculations (labeled RVM-2) are in excellent agreement with the data.

Since the calculated excitation cross section of the 4⁺ rotational state is insensitive to changes in the various E4 matrix elements, the rigid-rotor formula is used to relate all the hexadecapole matrix elements to $M_{04} = \langle 4^+ || M(E4) || 0^+ \rangle$.

TABLE I
Reduced transition matrix elements and charge deformation parameters in rare earth nuclei

Isotope	$\langle 2^+ M(E2) 0^+ \rangle$ (e · b)	$\langle 4^+ M(E4) 0^+ \rangle$ (e · b ²)	Fermi charge distr. ^{a)}		Homogeneous charge distr. ^{b)}	
			β_2	β_4	β_2	β_4
¹⁵⁰ Nd	1.650 ± 0.012	0.30 ^{+0.06} -0.07	0.267 ^{+0.006} -0.005	0.053 ^{+0.019} -0.022	0.241 ^{+0.006} -0.004	0.054 ^{+0.019} 0.022
¹⁵² Sm ^{c)}	1.864 ± 0.017	0.46 ± 0.08	0.278 ^{+0.007} -0.006	0.088 ^{+0.023} -0.024	0.250 ± 0.006	0.088 ± 0.023
¹⁵⁴ Sm ^{c)}	2.072 ± 0.010	0.57 ± 0.09	0.299 ^{+0.008} -0.007	0.105 ^{+0.025} -0.026	0.268 ^{+0.007} -0.008	0.104 ± 0.024
¹⁵⁴ Gd	1.958 ± 0.011	0.64 ^{+0.06} -0.07	0.268 ^{+0.006} -0.004	0.130 ^{+0.016} -0.019	0.240 ^{+0.006} -0.005	0.129 ^{+0.015} -0.019
¹⁵⁶ Gd	2.142 ± 0.020	0.41 ^{+0.12} -0.18	0.312 ^{+0.014} -0.010	0.055 ^{+0.033} -0.050	0.280 ^{+0.013} -0.009	0.056 ^{+0.031} -0.049

^{a)} $r_0 = 1.1$ fm, $a = 0.6$ fm.

^{b)} $r_0 = 1.2$ fm.

^{c)} Ref. 7).

The quadrupole and hexadecapole transition matrix elements obtained from the present study are listed in table 1. We find good agreement of our E2 and E4 matrix elements with previous results ^{1, 2, 5, 6}). In these earlier analyses the deviation of the $B(E2)$ values from the rigid-rotor prediction was taken into account by incorporating a "stretching" parameter for the nucleus ¹⁵²Sm, while for ¹⁵⁴Sm the rigid-rotor relationships were used to calculate the E2 matrix elements. Hexadecapole moments for the Gd isotopes have not thus far been studied by other authors. Also shown in table 1 are quadrupole (β_2) and hexadecapole (β_4) deformation parameters deduced from the reduced matrix elements (cf. the appendix) by using the relationship

$$\langle K = 0, n_2 = 0, n_0 = 0 | M'(E\lambda, 0) | K = 0, n_2 = 0, n_0 = 0 \rangle = \int \rho(r, \beta_2, \beta_4) r^\lambda Y_{\lambda 0}(\theta) d\tau. \quad (1)$$

The integral (1) was solved numerically for $\lambda = 2$ and 4 assuming two different models for the charge distribution. For a homogeneous charge density

$$\rho(r, \beta_2, \beta_4) = \begin{cases} \rho_0, & r \leq R(\theta) \\ 0, & r > R(\theta), \end{cases} \quad (2)$$

where the charge surface

$$R(\theta) = R_0 [1 + \beta_2 Y_{20}(\theta) + \beta_4 Y_{40}(\theta)]. \quad (3)$$

For the Fermi charge distribution the following form was used:

$$\rho(r, \beta_2, \beta_4) = \rho_0 [1 + \exp((r - R(\theta))/a)]^{-1}. \quad (4)$$

The integral (1) was normalized by adjusting ρ_0 to give the total nuclear charge $Ze = \int \rho(r, \beta_2, \beta_4) d\tau$, while both the radius parameter R_0 and the diffuseness a were held constant. For the Fermi distribution the radius was taken to be $R_0 = 1.1A^{1/3}$ fm and the diffuseness $a = 0.6$ fm, while for the homogeneous charge density $R_0 = 1.2A^{1/3}$ fm was used.

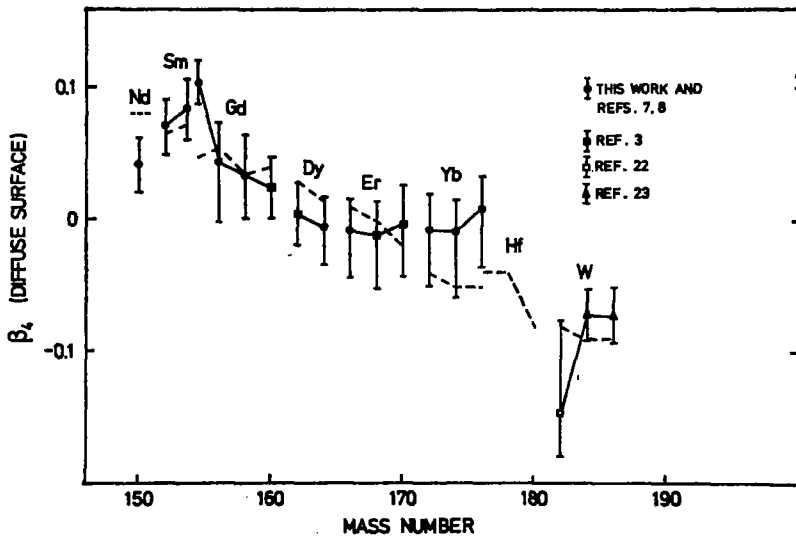


Fig. 3. Comparison between experimental β_4 values obtained for a Fermi charge distribution ($r_0 = 1.16$ fm, $a = 0.66$ fm) and the calculations of ref. ²¹) (dashed lines).

In fig. 3 the β_4 deformation parameters obtained for rare earth nuclei by Coulomb excitation measurements are summarized. To facilitate comparison with the theoretical values of Götz *et al.* ²¹), the nuclear radius was taken to be $R_0 = 1.16A^{1/3}$ fm and the diffuseness $a = 0.66$ fm.

The authors wish to thank Prof. W. Greiner and Prof. W. Scheid for stimulating discussions. Thanks are also due to the Hochschulrechenzentrum Frankfurt for providing the computing time necessary for the time consuming calculations.

Appendix

In this appendix we outline the derivation of the reduced E2 matrix element between ground-band rotational states in the transitional nuclei studied in this work. The rotation-vibration model of Faessler and Greiner¹⁵⁾ is used which includes the coupling of the ground state with both the $K^\pi = 2^+$ γ -vibrational and $K^\pi = 0^+$ β -vibrational degrees of freedom. The mixed wave function is expressed by

$$|\overline{IMKn_2n_0}\rangle = A_1(I)|IM000\rangle + A_2(I)|IM200\rangle + A_3(I)|IM001\rangle, \quad (\text{A.1})$$

where the amplitudes $A_i(I)$ are given in terms of the three rotation-vibration parameters ε , E_γ and E_β , of ref. 15). The unperturbed wave function is given by

$$|IMKn_2n_0\rangle = \left(\frac{2I+1}{16\pi^2} \frac{1}{1+\delta_{K0}} \right)^{\frac{1}{2}} (D_{MK}^I + (-)^I D_{M-K}^I) |Kn_2n_0\rangle. \quad (\text{A.2})$$

Here, $|Kn_2n_0\rangle$ denotes a vibrational state characterized by oscillator quantum numbers n_0 ($n_0 = 1$ for the $K^\pi = 0^+$ β -vibration) and n_2 ($n_2 = 0$ for the $K^\pi = 2^+$ γ -vibration). For the ground state $n_0 = n_2 = 0$. The calculation of the reduced E2 matrix element is now straightforward. Transforming the E2 operator $M(E2)$ to the body-fixed coordinate system and using the Wigner-Eckart theorem one obtains the E2 matrix element between ground-band states in terms of "intrinsic" interband and intraband matrix elements:

$$\begin{aligned} \langle I_f || M(E2) || I_i \rangle = & \sqrt{2I_i+1} \{ A_1(I_f) A_1(I_i) \langle I_i 200 | I_f 0 \rangle \langle 000 | M'(E2, 0) | 000 \rangle \\ & + A_1(I_f) A_2(I_i) \sqrt{2} \langle I_i 22 - 2 | I_f 0 \rangle \langle 000 | M'(E2, -2) | 200 \rangle \\ & + A_1(I_f) A_3(I_i) \langle I_i 200 | I_f 0 \rangle \langle 000 | M'(E2, 0) | 001 \rangle \\ & + A_2(I_f) A_1(I_i) \sqrt{2} \langle I_i 202 | I_f 2 \rangle \langle 200 | M'(E2, 2) | 000 \rangle \\ & + A_2(I_f) A_2(I_i) \langle I_i 220 | I_f 2 \rangle \langle 200 | M'(E2, 0) | 200 \rangle \\ & + A_2(I_f) A_3(I_i) \sqrt{2} \langle I_i 202 | I_f 2 \rangle \langle 200 | M'(E2, 2) | 001 \rangle \\ & + A_3(I_f) A_1(I_i) \langle I_i 200 | I_f 0 \rangle \langle 001 | M'(E2, 0) | 000 \rangle \\ & + A_3(I_f) A_2(I_i) \sqrt{2} \langle I_i 22 - 2 | I_f 0 \rangle \langle 001 | M'(E2, -2) | 200 \rangle \\ & + A_3(I_f) A_3(I_i) \langle I_i 200 | I_f 0 \rangle \langle 001 | M'(E2, 0) | 001 \rangle \}, \end{aligned} \quad (\text{A.3})$$

where the quantities $(I_i \lambda K_i \Delta K | I_f K_f)$ are Clebsch-Gordan coefficients. Eq. (A.3) can be simplified considerably by using the recent experimental results^{24, 25)} that for the nuclei studied in this work the quadrupole moments in the ground state, the $K^\pi = 0^+$ β -vibrational and $K^\pi = 2^+$ γ -vibrational states are equal. Moreover, since $A_2(I) \ll 1$ and $A_3(I) \ll 1$, contributions from transitions between the β - and γ -vibrational states can be neglected. Therefore, the reduced E2 matrix element can be written in terms of three "intrinsic" matrix elements, i.e. $\langle 000 | M'(E2, 0) | 000 \rangle$, $\langle 000 | M'(E2, -2) | 200 \rangle$ and $\langle 000 | M'(E2, 0) | 001 \rangle$, which, in turn, are obtained from the experimentally

measured quantities $B(E2; 0_{g.s.}^+ \rightarrow 2_{g.s.}^+)$, $B(E2; 0_{g.s.}^+ \rightarrow 2_7^+)$ and $B(E2; 0_{g.s.}^+ \rightarrow 2_f^+)$. In fig. 2, the $B(E2)$ values calculated from eq. (A.3) are compared with experimental results obtained for ^{152}Sm , ^{154}Sm , ^{154}Gd and ^{156}Gd .

References

- 1) F. S. Stephens, R. M. Diamond, N. K. Glendenning and J. de Boer, *Phys. Rev. Lett.* **24** (1970) 1137;
F. S. Stephens, R. M. Diamond and J. de Boer, *Phys. Rev. Lett.* **27** (1971) 1151
- 2) T. K. Saylor, J. X. Saladin, I. Y. Lee and K. A. Erb, *Phys. Lett.* **42B** (1972) 51
- 3) K. A. Erb, J. E. Holden, I. Y. Lee, J. X. Saladin and T. K. Saylor, *Phys. Rev. Lett.* **29** (1972) 1010
- 4) W. Ebert, P. Hecking, K. Pelz, S. G. Steadman and P. Winkler, *Z. Phys.* **263** (1973) 191
- 5) W. Brückner, J. G. Merdinger, D. Pelte, U. Smilansky and K. Traxel, *Phys. Rev. Lett.* **30** (1973) 57
- 6) A. H. Shaw and J. S. Greenberg, *Phys. Rev.* **C10** (1974) 263
- 7) H. J. Wollersheim, W. Wilcke, Th. W. Elze and D. Pelte, *Phys. Lett.* **48B** (1974) 323
- 8) H. J. Wollersheim, W. Wilcke and Th. W. Elze, *Phys. Rev.* **C11** (1975) 2008
- 9) C. E. Bemis, Jr., F. K. McGowan, J. L. C. Ford, Jr., W. T. Milner, P. H. Stelson and R. L. Robinson, *Phys. Rev.* **C8** (1973) 1466;
F. K. McGowan, C. E. Bemis, Jr., J. L. C. Ford, Jr., W. T. Milner, R. L. Robinson and P. H. Stelson, *Phys. Rev. Lett.* **27** (1971) 1741
- 10) C. Baktash and J. X. Saladin, *Phys. Rev.* **C10** (1974) 1136
- 11) J. H. Hamilton, L. Varnell, R. M. Ronningen, H. V. Ramayya, J. Lange, L. L. Reidinger, R. L. Robinson and P. H. Stelson, *Bull. Am. Phys. Soc.* **19** (1974) 579
- 12) H. J. Wollersheim and Th. W. Elze, *Verhandl. DPG (VI)* **10** (1975) 815
- 13) H. J. Wollersheim and Th. W. Elze, to be published
- 14) D. Pelte, private communication
- 15) A. Faessler, W. Greiner and R. K. Sheline, *Nucl. Phys.* **70** (1965) 33
- 16) A. S. Davydov and V. I. Ovcharenko, *Sov. J. Nucl. Phys.* **3** (1966) 740
- 17) A. S. Davydov, *Proc. Int. Conf. on nuclear structure, Tokyo 1967*, p. 133
- 18) R. M. Diamond, F. S. Stephens, K. Nakai and R. Nordhagen, *Phys. Rev.* **C3** (1971) 344
- 19) N. Rud, G. T. Ewan, A. Christy, D. Ward, R. L. Graham and J. S. Geiger, *Nucl. Phys.* **A191** (1972) 545
- 20) R. M. Diamond, G. D. Symons, J. L. Quebert, K. H. Maier, J. R. Leigh and F. S. Stephens, *Nucl. Phys.* **A184** (1972) 481
- 21) U. Götz, H. C. Pauli, K. Alder and K. Junker, *Nucl. Phys.* **A192** (1972) 1
- 22) C. E. Bemis, Jr., P. H. Stelson, F. K. McGowan, W. F. Milner, J. L. C. Ford, Jr., R. L. Robinson and W. Tuttle, *Phys. Rev.* **C8** (1973) 1934
- 23) I. Y. Lee, J. X. Saladin, C. Baktash, J. E. Holden and J. O'Brien, *Phys. Rev. Lett.* **33** (1974) 383
- 24) N. Rud, H. L. Nielsen and K. Wilaky, *Nucl. Phys.* **A167** (1971) 401
- 25) C. W. Reich and I. E. Cline, *Nucl. Phys.* **A169** (1970) 181